

# **Engineered Covers for Waste Containment: Changes in Engineering Properties and Implications for Long-Term Performance Assessment – Appendices**

**AVAILABILITY OF REFERENCE MATERIALS  
IN NRC PUBLICATIONS**

**NRC Reference Material**

As of November 1999, you may electronically access NUREG-series publications and other NRC records at NRC's Public Electronic Reading Room at <http://www.nrc.gov/reading-rm.html>. Publicly released records include, to name a few, NUREG-series publications; *Federal Register* notices; applicant, licensee, and vendor documents and correspondence; NRC correspondence and internal memoranda; bulletins and information notices; inspection and investigative reports; licensee event reports; and Commission papers and their attachments.

NRC publications in the NUREG series, NRC regulations, and *Title 10, Energy*, in the Code of *Federal Regulations* may also be purchased from one of these two sources.

1. The Superintendent of Documents  
U.S. Government Printing Office  
Mail Stop SSOP  
Washington, DC 20402-0001  
Internet: [bookstore.gpo.gov](http://bookstore.gpo.gov)  
Telephone: 202-512-1800  
Fax: 202-512-2250
2. The National Technical Information Service  
Springfield, VA 22161-0002  
[www.ntis.gov](http://www.ntis.gov)  
1-800-553-6847 or, locally, 703-605-6000

A single copy of each NRC draft report for comment is available free, to the extent of supply, upon written request as follows:

Address: U.S. Nuclear Regulatory Commission  
Office of Administration  
Publications Branch  
Washington, DC 20555-0001

E-mail: [DISTRIBUTION.RESOURCE@nrc.gov](mailto:DISTRIBUTION.RESOURCE@nrc.gov)  
Facsimile: 301-415-2289

Some publications in the NUREG series that are posted at NRC's Web site address <http://www.nrc.gov/reading-rm/doc-collections/nuregs> are updated periodically and may differ from the last printed version. Although references to material found on a Web site bear the date the material was accessed, the material available on the date cited may subsequently be removed from the site.

**Non-NRC Reference Material**

Documents available from public and special technical libraries include all open literature items, such as books, journal articles, and transactions, *Federal Register* notices, Federal and State legislation, and congressional reports. Such documents as theses, dissertations, foreign reports and translations, and non-NRC conference proceedings may be purchased from their sponsoring organization.

Copies of industry codes and standards used in a substantive manner in the NRC regulatory process are maintained at—

The NRC Technical Library  
Two White Flint North  
11545 Rockville Pike  
Rockville, MD 20852-2738

These standards are available in the library for reference use by the public. Codes and standards are usually copyrighted and may be purchased from the originating organization or, if they are American National Standards, from—

American National Standards Institute  
11 West 42<sup>nd</sup> Street  
New York, NY 10036-8002  
[www.ansi.org](http://www.ansi.org)  
212-642-4900

Legally binding regulatory requirements are stated only in laws; NRC regulations; licenses, including technical specifications; or orders, not in NUREG-series publications. The views expressed in contractor-prepared publications in this series are not necessarily those of the NRC.

The NUREG series comprises (1) technical and administrative reports and books prepared by the staff (NUREG-XXXX) or agency contractors (NUREG/CR-XXXX), (2) proceedings of conferences (NUREG/CP-XXXX), (3) reports resulting from international agreements (NUREG/IA-XXXX), (4) brochures (NUREG/BR-XXXX), and (5) compilations of legal decisions and orders of the Commission and Atomic and Safety Licensing Boards and of Directors' decisions under Section 2.206 of NRC's regulations (NUREG-0750).

**DISCLAIMER:** This report was prepared as an account of work sponsored by an agency of the U.S. Government. Neither the U.S. Government nor any agency thereof, nor any employee, makes any warranty, expressed or implied, or assumes any legal liability or responsibility for any third party's use, or the results of such use, of any information, apparatus, product, or process disclosed in this publication, or represents that its use by such third party would not infringe privately owned rights.

# **Engineered Covers for Waste Containment: Changes in Engineering Properties and Implications for Long-Term Performance Assessment – Appendices**

Prepared by:

C.H.Benson<sup>1</sup>, W.H. Albright<sup>2</sup>, D.O. Fratta<sup>1</sup>, J.M. Tinjum<sup>1</sup>,  
E. Kucukkirca<sup>1</sup>, S.H. Lee<sup>1</sup>, J. Scalia<sup>1</sup>, P.D. Schlicht<sup>1</sup>, and X. Wang<sup>1</sup>,

<sup>1</sup>Geological Engineering  
University of Wisconsin-Madison  
1415 Engineering Drive  
Madison, WI 53706

<sup>2</sup>Desert Research Institute  
2215 Raggio Parkway  
Reno, NV 89512

Manuscript Completed: July 2010  
Date Published: December 2011

Jacob Philip, NRC Project Manager

NRC Job Code N6366

Office of Nuclear Regulatory Research



## ABSTRACT

This peer-reviewed study demonstrates that engineering properties of cover soils change while in service and that long-term engineering properties should be used as input to models employed for performance assessments. Recommendations for appropriate input are made based on the data that were collected. Increases in the saturated hydraulic conductivity, saturated volumetric water content, and the air entry suction (as characterized by van Genuchten's  $\alpha$  parameter) occurred due to formation of soil structure, regardless of climate, cover design, or service life. Substantial changes in hydraulic conductivity were observed in some geosynthetic clay liners (GCLs) that did not hydrate completely and underwent cation exchange. Changes in geomembranes and geosynthetic drainage layers were modest or small, and computations based on antioxidant depletion rates suggest that the minimum service life of geomembranes is on the order of 50-125 yrs (the actual service life will be longer). The findings indicate that covers should be monitored to ensure that they are functioning as intended. Monitoring using pan lysimeters combined with secondary measurements collected for interpretive purposes is recommended. Future research investments should include an evaluation of remote sensing technologies for cover monitoring and analog studies to estimate properties of earthen and geosynthetic cover materials corresponding to service lives of 100s to 1000s of years.



# CONTENTS

|  |      |
|--|------|
| Abstract.....  | iii  |
| Executive Summary .....  | xv   |
| Acknowledgement.....   | xvii |
| Abbreviations .....  | xix  |
| 1. Introduction .....  | 1-1  |
| 2. Background: ACAP Test Sections.....                                   | 2-1  |
| 2.1 ACAP Lysimeters.....   | 2-6  |
| 2.2 Data Collection.....   | 2-6  |
| 2.3 Calibration and Data Quality Control.....                            | 2-8  |
| 2.4 Cover Soils.....   | 2-8  |
| 2.5 Geosynthetics.....   | 2-8  |
| 3. Exhumations .....   | 3-1  |
| 3.1 Soil Sampling and Field Testing .....                                | 3-1  |
| 3.2 Sampling of Geosynthetics .....                                      | 3-6  |
| 3.3 Geomorphological Surveys.....  | 3-6  |
| 3.4 Geophysical Surveys .....  | 3-6  |
| 4. Field Test Methods.....   | 4-1  |
| 4.1 Sealed Double-Ring Infiltrometer Tests .....                         | 4-1  |
| 4.2 Borehole Tests .....   | 4-1  |
| 4.3 Hydraulic Conductivity from Peak Lysimeter Flow Rates .....          | 4-2  |
| 5. Laboratory Test Methods .....   | 5-1  |
| 5.1 Hydraulic Properties of Earthen Materials.....                       | 5-1  |
| 5.2 Properties of Geosynthetic Clay Liners.....                          | 5-1  |
| 5.2.1 Saturated Hydraulic Conductivity .....                             | 5-1  |
| 5.2.2 Swell Index .....  | 5-2  |
| 5.2.3 Soluble Cations, Bound Cations, and Cation Exchange Capacity ..... | 5-2  |
| 5.2.4 Subgrade Soils .....   | 5-3  |
| 5.3 Properties of Geomembranes and Geosynthetic Drainage Layers .....    | 5-3  |
| 5.3.1 Tensile Strength of Geomembranes .....                             | 5-3  |
| 5.3.2 Ply Adhesion of Geosynthetic Drainage Layers .....                 | 5-3  |
| 5.3.3 Interface Shear Strength .....                                     | 5-3  |
| 5.3.4 Hydraulic Properties .....   | 5-4  |
| 5.3.5 Melt Flow Index and Oxidation Induction Time .....                 | 5-4  |
| 6. Earthen Barrier and Storage Layers.....                               | 6-1  |
| 6.1 Soil Characteristics.....  | 6-1  |
| 6.2 Field Hydraulic Conductivity .....                                   | 6-6  |
| 6.3 Laboratory Hydraulic Conductivity .....                              | 6-10 |
| 6.4 Comparison of In-Service and As-Built Hydraulic Conductivity .....   | 6-12 |
| 6.5 Factors Affecting Changes in Hydraulic Conductivity .....            | 6-18 |

|   |       |
|---|-------|
| 6.5.1 Service Life .....  | 6-18  |
| 6.5.2 Climate .....   | 6-18  |
| 6.5.3 Soil Composition .....  | 6-22  |
| 6.5.4 Compaction Conditions .....   | 6-22  |
| 6.5.5 Effect of Freeze-Thaw and Wet-Dry Cycles .....                                | 6-28  |
| 6.6 Soil Water Characteristic Curves .....  | 6-31  |
| 6.7 Summary of Findings for Earthen Storage and Barrier Layers .....                | 6-38  |
| 7. Geosynthetic Clay Liners .....   | 7-1   |
| 7.1 Background on GCLs .....  | 7-3   |
| 7.2 Properties of Exhumed GCLs .....  | 7-4   |
| 7.2.1 GCL Water Content and Cation Exchange .....                                   | 7-4   |
| 7.2.2 Hydraulic Conductivity .....  | 7-8   |
| 7.2.3 Effect of Subgrade Condition .....  | 7-11  |
| 7.2.4 Service Life and Cover Soil Thickness .....                                   | 7-15  |
| 7.3 Key Factors to Successful GCL Performance .....                                 | 7-15  |
| 7.4 Summary of Findings for GCLs .....  | 7-22  |
| 8. Geomembranes and Geosynthetic Drainage Layers .....                              | 8-1   |
| 8.1 Properties of Geomembranes .....  | 8-1   |
| 8.1.1 Tensile Strength .....  | 8-1   |
| 8.1.2 OIT and MFI .....   | 8-6   |
| 8.2 Properties of Geocomposite Drainage Layer .....                                 | 8-11  |
| 8.2.1 Transmissivity .....  | 8-11  |
| 8.2.2 Permittivity .....  | 8-16  |
| 8.2.3 Ply Adhesion .....  | 8-16  |
| 8.3 Interface Shear Strength .....  | 8-21  |
| 8.4 Reduction Factors for Design .....  | 8-21  |
| 8.5 Summary of Findings for Geomembranes and Drainage Layers .....                  | 8-26  |
| 9. Geophysical Evaluation .....   | 9-1   |
| 9.1 Electrical Resistivity Surveys .....  | 9-1   |
| 9.2 Ground Penetrating Radar Surveys .....  | 9-8   |
| 9.3 Summary of Findings from Geophysical Surveys .....                              | 9-15  |
| 10. Practical Implications for Design, Performance Assessment, and Monitoring ..... | 10-1  |
| 10.1 Design Conditions .....  | 10-2  |
| 10.2 Parameters for Performance Assessments .....                                   | 10-3  |
| 10.3 Monitoring .....   | 10-4  |
| 10.3.1 Performance Monitoring .....   | 10-5  |
| 10.3.2 Interpretive Monitoring .....  | 10-8  |
| 10.3.3 Recommended Practice for Final Cover Monitoring .....                        | 10-11 |
| 11. Conclusions and Recommendations .....   | 11-1  |
| 12. References .....  | 12-1  |
| Appendices (Volume 2)   |       |
| Appendix A Exhumation Photo Gallery .....   | A-1   |
| Appendix B Sealed Double-Ring Infiltrometer (SDRI) Data .....                       | B-1   |
| Appendix C TSB Data .....   | C-1   |



|            |   |     |
|------------|---|-----|
| Appendix D | Laboratory Hydraulic Conductivity Data .....  | D-1 |
| Appendix E | Soil Water Characteristic Curve Test Data .....   | E-1 |
| Appendix F | Statistical Analyses of Hydraulic Conductivity Data .....   | F-1 |
| Appendix G | Methods Used in Chemical Analyses of Geosynthetic<br>Clay Liners .....  | G-1 |
| Appendix H | Test Methods for Measuring Soluble Cations, Bound Cations,<br>and Cation Exchange Capacity .....                    | H-1 |
| Appendix I | Schematic and Photograph of Hydraulic Conductivity Test Set-Up<br>for Geosynthetic Clay Liners (GCLs) .....         | I-1 |
| Appendix J | Exhumed Subgrade Porewater Chemistries .....  | J-1 |
| Appendix K | Exhumed GCLs Water Content, Bound Cations, and<br>Soluble Cations .....   | K-1 |
| Appendix L | Hydraulic Conductivity Records for Exhumed GCLs .....   | L-1 |
| Appendix M | Field Exhumation Photographs and Observations .....   | M-1 |
| Appendix N | Laboratory Testing Photography and Observations .....   | N-1 |
| Appendix O | Exploration of GCL Laboratory Testing Methods .....   | O-1 |
| Appendix P | Supplemental Graphs and Tables from Geosynthetic Membrane<br>(GM) and Geosynthetic Drainage Layer (GDL) Tests ..... | P-1 |
| Appendix Q | Photographs of GM and GDL Testing Data .....  | Q-1 |
| Appendix R | GM Test Data .....  | R-1 |
| Appendix S | GDL Test Data .....   | S-1 |

## List of Figures

|            |  |      |
|------------|--|------|
| Fig. 2.1.  | Locations of ACAP field sites. Sites exhumed in this study marked with a star.   | 2-2  |
| Fig. 2.2.  | Profiles of conventional covers evaluated by ACAP.   | 2-3  |
| Fig. 2.3.  | Profiles of store-and-release covers evaluated by ACAP.  | 2-4  |
| Fig. 2.4.  | Schematic of ACAP lysimeter (not to scale).  | 2-7  |
| Fig. 3.1.  | Profiles of the final covers at full-scale MSW landfills in Wisconsin (Site E) and Michigan (Site F). GDL = geosynthetic drainage layer, GM = geomembrane, and GCL = geosynthetic clay liner. Service life of Wisconsin site is 4.7-5.8 yr (depending on test pit). Service life of Michigan site is 3.1 yr. | 3-2  |
| Fig. 3.2.  | BH test conducted during exhumation of ACAP test section in Helena, MT.  | 3-3  |
| Fig. 3.3.  | SDRI test conducted at ACAP test facility in Polson, MT. Upper photograph shows inner and outer rings after installation. Lower photograph shows filled SDRI with Mariotte bottle in the rear.   | 3-4  |
| Fig. 3.4.  | Block sample being collected at ACAP test facility in Underwood, ND. Upper photograph shows sample partially trimmed into ring. Lower photograph shows sample in ring and ready for separation from subgrade.  | 3-5  |
| Fig. 3.5.  | Removing cover soils over a composite barrier layer (a) and removing a sample of geosynthetic drainage layer (b). Both photographs are from final cover at Wisconsin MSW landfill.   | 3-7  |
| Fig. 3.6.  | Exhumation of GCL samples: cutting around perimeter with razor knife (a) and delicately sliding sample onto rigid plastic plate (b).   | 3-8  |
| Fig. 3.7.  | Typical setup for evaluating punctures in geomembranes using electrical resistivity measurements (after Frangos 1997, Darilek and Miller 1998).  | 3-9  |
| Fig. 3.8.  | Typical voltage drop over a hole in a geomembrane hole: experimental measurements and theoretical response (from Parra 1988).  | 3-11 |
| Fig. 3.9.  | Common mid-point (a) and reflection survey (b) setup configuration for GPR.  | 3-12 |
| Fig. 3.10. | Downhole setup for GPR.  | 3-13 |
| Fig. 6.1.  | Plasticity chart showing Atterberg limits of storage and barrier layers evaluated in this study.   | 6-3  |
| Fig. 6.2.  | Field hydraulic conductivity determined by SDRIs and BHs from each cover type (a) and hydraulic conductivity from SDRIs versus hydraulic conductivity from BHs for individual test sections (b).   | 6-8  |

|            |  |      |
|------------|--|------|
| Fig. 6.3.  | Saturated hydraulic conductivity from SDRI and BH tests (a) and laboratory tests on 305, 150 and 75 mm diameter specimens for each cover type (b). The solid line within the box represents the median, the box encloses 50% of the data, and outliers are indicated with a circle. .... | 6-9  |
| Fig. 6.4.  | Saturated hydraulic conductivity of large-scale (305 mm) laboratory specimens versus small-scale (150 and 75-mm-diameter) laboratory specimens. ....   | 6-13 |
| Fig. 6.5.  | Field hydraulic conductivity from SDRI and BH versus large-scale (305 mm) laboratory saturated hydraulic conductivity (a) and small scale (150 and 75-mm) laboratory saturated hydraulic conductivity (b). ....  | 6-14 |
| Fig. 6.6.  | Saturated hydraulic conductivity versus effective diameter for t Altamont store-and-release cover (a) and Apple Valley clay barrier (b). Trend lines drawn by hand. ....   | 6-15 |
| Fig. 6.7.  | In-service saturated hydraulic conductivity ( $K_{si}$ ) versus as-built hydraulic conductivity ( $K_{sa}$ ) by site (a) and cover type (b). “?” signifies apparent outliers. ....   | 6-17 |
| Fig. 6.8.  | Saturated hydraulic conductivity ratio ( $K_{si}/K_{sa}$ ) versus as-built saturated hydraulic conductivity ( $K_{sa}$ ). Trend lines drawn by hand. “?” signifies outliers. ....  | 6-19 |
| Fig. 6.9.  | Saturated hydraulic conductivity ratio versus service life of test section. Trend lines drawn by hand. ....  | 6-20 |
| Fig. 6.10. | Saturated hydraulic conductivity ratio versus climate presented by cover type. ....  | 6-21 |
| Fig. 6.11. | Saturated hydraulic conductivity ratio versus plasticity index (a), clay content ( $< 2 \mu\text{m}$ ) (b), and activity (c). PI = 0 indicates soil is non plastic. .  | 6-23 |
| Fig. 6.12. | Saturated hydraulic conductivity versus coarse fraction ( $\% > 75 \mu\text{m}$ ) over clay content ( $\% < 2 \mu\text{m}$ ) (a) and ratio of silt content ( $\%$ between 2 and 75 $\mu\text{m}$ ) to fines content ( $\% < 75 \mu\text{m}$ ) (b). ....                                  | 6-25 |
| Fig. 6.13. | Saturated hydraulic conductivity ratio versus as-built compacted dry unit weight by site (a) and cover type (b). ....  | 6-27 |
| Fig. 6.14. | Saturated hydraulic conductivity ratio versus water content relative to optimum water content. ....  | 6-29 |
| Fig. 6.15. | Saturated hydraulic conductivity ratio versus number of freeze-thaw cycles (a) and number of wet-dry cycles (b). ....  | 6-30 |
| Fig. 6.16. | In-service $\alpha$ parameter versus as-built $\alpha$ parameter (a) and in-service n parameter versus as-built n parameter (b). ....  | 6-35 |

|            |   |      |
|------------|---|------|
| Fig. 6.17. | In-service saturated volumetric water content versus as-built saturated volumetric water content. ....  | 6-36 |
| Fig. 6.18. | The ratio of $\alpha$ (a) and $n$ (b) from large-scale testing (254 or 150 mm) to small scale testing (75 mm). ....   | 6-37 |
| Fig. 7.1.  | Profiles of final covers evaluated by Meer and Benson (2007). The service life varied from 4.1 to 11.1 yr. ....   | 7-2  |
| Fig. 7.2.  | Swell index in DW (a) and mole fraction monovalent bound cations (b) for GCL-only and composite GCL covers. Data are from this study (open symbols) and Meer and Benson (2007) (closed symbols). ....   | 7-7  |
| Fig. 7.3.  | Water content of exhumed GCLs (a) and subgrades (b) for covers where GCLs were in composite barriers or the sole barrier layer. Data are from this study (open symbols) and Meer and Benson (2007) (closed symbols). ....   | 7-9  |
| Fig. 7.4.  | Hydraulic conductivity of exhumed GCLs from covers where GCLs were in composite barriers or the sole barrier layer. Data are from this study (open symbols) and Meer and Benson (2007) (closed symbols). Circles represent hydraulic conductivity to SW; shaded boxes represent hydraulic conductivity to DW. GCLs permeated with DW at Wisconsin site (W-02) are duplicates of GCLs that had high hydraulic conductivity to SW. .... | 7-10 |
| Fig. 7.5   | Hydraulic conductivity versus (a) swell index in DW and (b) mole fraction bound sodium for exhumed GCLs from composite barriers. Data for new GCL are from Meer and Benson (2007). ....   | 7-12 |
| Fig. 7.6.  | Hydraulic conductivity of exhumed GCLs vs. water content (a) and water content of exhumed GCLs versus corresponding water content of subgrade (b). GCLs with lower $K$ had hydraulic conductivities $< 5 \times 10^{-11}$ m/s, whereas GCLs with higher $K$ had hydraulic conductivities $> 1 \times 10^{-9}$ m/s. ....   | 7-13 |
| Fig. 7.7.  | TCM (a) and $X_m$ (b) of GCL versus water content of subgrade. GCLs with lower $K$ had hydraulic conductivities $< 5 \times 10^{-11}$ m/s, whereas GCLs with higher $K$ had hydraulic conductivities $> 1 \times 10^{-9}$ m/s. ....   | 7-14 |
| Fig. 7.8.  | TCM of GCL vs. TCM of subgrade (a) and MDR of GCL vs. MDR of subgrade (b). GCLs with lower $K$ had hydraulic conductivities $< 5 \times 10^{-11}$ m/s, whereas GCLs with higher $K$ had hydraulic conductivities $> 1 \times 10^{-9}$ m/s. ....   | 7-16 |
| Fig. 7.9.  | Hydraulic conductivities of GCLs exhumed in this study as a function of USCS classification of subgrade. Compilation of data from Meer and Benson (2007) Site S and from this study. ....   | 7-17 |
| Fig. 7.10. | Hydraulic conductivity of exhumed GCLs permeated with SW and DW vs. service life (a) and thickness of overlying soil (b). Data are from this study and Site S in Meer and Benson (2007). ....   | 7-18 |

|            |  |      |
|------------|--|------|
| Fig. 7.11. | Cross-sections of exhumed GCLs from Site E-02 (a) and Site B (b). Vertical scale in mm. ....   | 7-20 |
| Fig. 7.12. | Cross-sections of exhumed GCLs from Site S (a) and Site F-03 (b). Photo of GCL from Site S is from Meer (2004). Photo of GCL from Site F-03 is from after permeation with rhodamine WT dye. Vertical scale in mm. ....   | 7-21 |
| Fig. 8.1.  | Profiles of covers at sites where geosynthetics were exhumed. GCL = geosynthetic clay liner, GDL = geosynthetic drainage layer, GM = geomembrane, GX = geotextile, RB = root barrier. ....   | 8-2  |
| Fig. 8.2.  | Narrow strip break strengths for the geomembrane samples. Horizontal bars in each column represent the average for the data in the column. Polymer types are noted at the top of each column. Two headed arrows represent manufacturer's MARV. ....  | 8-4  |
| Fig. 8.3.  | Strains at narrow strip yield strength (a) and break strength (b). Horizontal bars in each column represent the average for the data in the column. Two headed arrows represent manufacturers' MARV. ....  | 8-5  |
| Fig. 8.4   | Comparison between narrow-strip and wide-strip yield strengths (a) and narrow strip break and narrow strip yield strengths (b). ....   | 8-7  |
| Fig. 8.5.  | Oxidation induction time (OIT) (a) and melt flow index (MFI) (b) for the geomembrane. OIT and MFI were measured by TRI Environmental, Inc. of Austin, Texas. Horizontal bars in each column represent the average for the data in the column. Solid line at 130 min in OIT graph represents the manufacturers' MARV. Two headed arrows represent the OIT estimates of the exhumed samples calculated by the Arrhenius equation. .... | 8-9  |
| Fig. 8.6.  | OIT of exhumed geomembranes normalized by MARV and OIT as a function of time. $OIT_e$ = exhumed OIT. $OIT_o$ = MARV OIT. ....  | 8-10 |
| Fig. 8.7.  | Transmissivity of GDL under normal stress of 24 kPa (a) and 480 kPa (b). Horizontal bars in each column represent the average for data in the column.....  | 8-13 |
| Fig. 8.8   | Transmissivity of exhumed GDLs as a function of stress and MARV transmissivities for Altamont (a), Boardman (b), Cedar Rapids (c), and Omaha (d). ....   | 8-14 |
| Fig. 8.9.  | Site average transmissivity of GDL as a function of percent fines of the cover soil. Error bars represent one standard deviation from the mean. ..   | 8-15 |
| Fig. 8.10. | Permittivity of GDL using 10 mm head (a) and 50 mm head (b). Horizontal bars in each column represent the average for the data in the column. Two headed arrows represent manufacturers' MARV. ....  | 8-17 |
| Fig. 8.11. | Site average permittivity as a function of percent fines of the cover soil. Error bars represent one standard deviation from the mean. ....  | 8-18 |

|   |      |
|---|------|
| Fig. 8.12. Ply adhesion of GDL. Horizontal bars in each column represent the average the average for the data in the column. Two headed arrows represent manufacturers' MARV. ....  | 8-19 |
| Fig. 8.13. Site average ply adhesion as a function of service life (a) and number of freeze- thaw cycles (b). Error bars represent one standard deviation from = mean. ....   | 8-22 |
| Fig. 8.14. Peak interface shear strength envelope of GM-GDL interface for geosynthetics sampled from the Wisconsin site. ....   | 8-24 |
| Fig. 9.1. Configuration for the electrical resistivity survey used at the Altamont site.  | 9-2  |
| Fig. 9.2. Placement of current electrode under the GM at the Altamont site. ....  | 9-3  |
| Fig. 9.3. Raw (a) and smoothed (b) distribution of voltage drop from electrical resistivity survey of conventional cover at Altamont site (scale in mV). ....   | 9-4  |
| Fig. 9.4. Contour (a) and surface plots (b) of electrical resistivity data from conventional cover at Polson site. Suspect areas marked with red circles and location of intentional defect shown with solid yellow circle. ....  | 9-5  |
| Fig. 9.5. Contour and surface plots of electrical resistivity survey of conventional cover at Omaha site (more detailed maps are presented on right). Suspect areas are marked with red oval; green box shows location of gash in GM in Fig. 9.6 (voltage amplitudes in mV). .... | 9-6  |
| Fig. 9.6. Gash in GM at Omaha site that was detected from electrical resistivity survey (lip balm container shown for scale). ....  | 9-7  |
| Fig. 9.7. Antennae (200 MHz) used for GPR surveys at Altamont and Omaha sites.  | 9-9  |
| Fig. 9.8. GPR reflection survey at Altamont site along survey line in Fig. 9.1. Profile shows both point reflector above ground (e.g., tools, cables, etc. on surface) and below ground (sensor cables, etc.).....  | 9-10 |
| Fig. 9.9. EM wave traces collected along survey line shown in Fig. 9.1. ....  | 9-11 |
| Fig. 9.10. Tomographic images of EM wave velocity at Altamont site. ....  | 9-12 |
| Fig. 9.11. GPR reflection survey across all three cover sections at Omaha site. ....  | 9-13 |
| Fig. 9.12. Photograph of thick store-and-release cover at Omaha site showing thick upper storage layer, sand layer for capillary break (white layer), and lower interim cover layer. Note uniformity of layers and moist condition of storage layer and topsoil. ....             | 9-14 |
| Fig. 9.13. Tomographic images of downhole EM wave velocity from the thick store-and-release cover at the Omaha site. ....   | 9-16 |

|            |  |       |
|------------|--|-------|
| Fig. 10.1  | Daily precipitation and percolation record (a) and water content vs. time at various depths (b) in first quarter of 1995 for the final cover test section in Wenatchee, WA described in Khire et al. (1997).....   | 10-6  |
| Fig. 10.2  | Schematic of flux meter used to monitor a final cover (adapted from Malusis and Benson 2006). .....  | 10-7  |
| Fig. 10.3  | Storage and percolation (a) and water contents at various depths (b) as a function of time for thin store-and-release cover evaluated by ACAP in Sacramento, CA. ....  | 10-10 |
| Fig. 10.4. | Typical profile of a sensor nest used for interpretive data (adapted from Benson et al. 2009). Labels to right of profile describe layers in cover profile. No sensors were placed in rip rap layer due to the large particle sizes and the negligible storage anticipated in this layer. .... | 10-12 |
| Fig. 10.5. | Moderate frequency TDR sensor ready to be pushed into cover profile. Type-T thermocouple (blue wire) is taped head of TDR sensor. ....   | 10-13 |
| Fig. 10.6  | Water balance quantities for ACAP test sections near Grand Junction, CO (from Benson et al. 2009). ....  | 10-15 |
| Fig. 10.7. | Water contents in frost protection layer and radon barrier measured at same depth in up slope and down slope nests of Test Section A (adapted from Benson et al. 2009). ....   | 10-17 |
| Fig. 10.8. | Comparison of water contents in frost protection layer in upslope (Probe 5) and down slope (Probe 12) interpretive monitoring nests in duplicate test sections (Test Sections A and B). ....   | 10-18 |

## List of Tables

|             |  |      |
|-------------|--|------|
| Table 2.1.  | Climatic characteristics and slopes of ACAP sites. ....  | 2-5  |
| Table 6.1.  | Site characteristics and soil index properties for storage and barrier layers evaluated in this study. ....                        | 6-2  |
| Table 6.2.  | Average as-built compaction and water content for storage and barrier layers evaluated in this study. ....                         | 6-4  |
| Table 6.3.  | As-built hydraulic properties for storage and barrier layers evaluated in this study. ....   | 6-5  |
| Table 6.4.  | Field hydraulic conductivity for storage and barrier layers. ....  | 6-7  |
| Table 6.5.  | Saturated hydraulic conductivity measured in laboratory on specimens from in-service storage and barrier layers. ....              | 6-11 |
| Table 6.6.  | In-service saturated hydraulic conductivity for storage and barrier. ....  | 6-16 |
| Table 6.7.  | In-service dry unit weight and relative compaction for storage layers. ...   | 6-26 |
| Table 6.8.  | SWCC parameters for storage and barrier layers from 75-mm-diameter specimens. ....   | 6-32 |
| Table 6.9.  | SWCC parameters for storage and barrier layers from 150-mm-diameter specimens. ....  | 6-33 |
| Table 6.10. | SWCC parameters for storage and barrier layers from 254-mm-diameter specimens. ....  | 6-34 |
| Table 7.1.  | Physical and chemical properties of exhumed GCLs. ....   | 7-5  |
| Table 7.2.  | Water Content, TCM, and MDR of exhumed GCLs. ....  | 7-6  |
| Table 7.3.  | USCS Classification and Arithmetic Mean Water Content, TCM, and MDR of Subgrade Soils. ....  | 7-6  |
| Table 8.1.  | Tensile properties of exhumed GMs (average reported, range of property in parenthesis). ....                                       | 8-3  |
| Table 8.2.  | Melt flow index (MFI) and oxidation induction time (OIT) of exhumed GMs (average reported, range of property in parenthesis). .... | 8-8  |
| Table 8.3.  | Transmissivities and permittivities of exhumed GDLs (average reported, range of property in parenthesis). ....                     | 8-12 |



|             |  |       |
|-------------|--|-------|
| Table 8.4.  | Ply adhesions of exhumed GDLs (average reported range of property in parenthesis).....   | 8-20  |
| Table 8.5   | Shear strength parameters for the interface between the exhumed GDLs and GMs (average reported, range of property in parenthesis). ..... | 8-23  |
| Table 8.6   | Summary of reduction factors from previous studies and current study of exhumed geosynthetics. ....                                      | 8-25  |
| Table 10.1. | Water balance quantities for two ACAP test sections near Grand Junction, CO (from Benson et al. 2009). ....                              | 10-16 |



## EXECUTIVE SUMMARY

In this peer-reviewed study, final covers at test facilities and operating waste containment facilities were exhumed to evaluate how the properties of the cover materials changed 4.0-8.9 yr after installation (6.3 yr on average). Field tests were conducted, samples were collected, laboratory testing was performed, and data analyses were conducted. The findings demonstrate that engineering properties of cover soils change while in service and that long-term engineering properties should be used as input to models employed for performance assessments. Recommendations for appropriate input are made based on the data that were collected.

Changes in hydraulic properties occurred in all cover soils evaluated due to the formation of soil structure, regardless of climate, cover design, or service life. The saturated hydraulic conductivity and the  $\alpha$  parameter for the soil water characteristic curve (SWCC) increased, which reflects formation of larger pores due to pedogenic processes such as wet-dry and freeze-thaw cycling. Larger changes were observed for soils with lower as-built saturated hydraulic conductivity and soils with a greater proportion of clay particles in the fines fraction. Hydraulic properties of the cover soils were similar when exhumed, regardless of the as-built condition. Test scale had a significant effect on the hydraulic properties, with conditions near field-scale obtained using 0.3-m test specimens.

Substantial changes were also observed in some geosynthetic clay liners (GCLs). Analysis showed that GCLs have very low saturated hydraulic conductivity ( $< 5 \times 10^{-11}$  m/s) when placed on a moist subgrade (water content  $> 10\%$ ) and covered with a geomembrane and cover soil soon after installation. GCLs installed under other conditions can be much more permeable. GCLs that underwent and maintained complete hydration with osmotic swell retained low hydraulic conductivity even when Na was replaced by Ca and Mg provided they did not dehydrate. GCLs that undergo osmotic swell and are covered with a geomembrane surcharged with cover soils are expected to retain low hydraulic conductivity provided the geomembrane remains intact.

Changes in geomembranes and geosynthetic drainage layers were modest or small. Analysis of antioxidants in geomembranes showed that antioxidant depletion was reasonably consistent with expectations based on first-order kinetics and laboratory-measured depletion rates. Based on antioxidant depletion, the minimum service life of geomembranes is on the order of 50-125 yrs. Actual service lives may be longer but are difficult to predict based on the limited information available today.

Because changes in the engineering properties of cover materials are commonplace, and significant in some cases, monitoring of covers should be conducted to ensure they are functioning as intended. Monitoring using pan lysimeters combined with secondary measurements collected for interpretive purposes (water content, temperature, vegetation surveys, etc.) is recommended. Future research investments should explore how remote sensing technologies can be used for cover monitoring.

This study represents a snap shot in the evolution of final covers approximately 5 to 10 yr after construction. Additional research investments are needed to more accurately and completely define very long-term properties of earthen and geosynthetic cover materials corresponding to 100s or 1000s of years. These research investments should include analog studies of natural environments where earthen and natural polymeric materials exist as well as accelerated laboratory experiments that can be used to develop predictive degradation models.



## **ACKNOWLEDGEMENT**

This research study was funded by a consortium consisting of the U.S. Nuclear Regulatory Commission's Office of Nuclear Regulatory Research (through a grant to the University of Wisconsin-Madison Water Resources Institute under an interagency agreement, IA-RES-08-132, with the U. S. Geological Survey State Water Resources Research Institute Program), the National Science Foundation (Grant No. CMMI-0625850), the U.S. Environmental Protection Agency, the U.S. Department of Energy, the Environmental Research and Education Foundation, Colloid Environmental Technologies Corporation, Veolia Environmental Services, and Waste Connections, Inc. This support is gratefully acknowledged.

The research report was peer reviewed by an expert panel consisting of Charles D. Shackelford, John D. McCartney, and George R. Koerner. The authors of the research report considered and incorporated their comments and suggestions when finalizing the report.



## ABBREVIATIONS

### Acronyms

|                |   |
|----------------|---|
| ACAP           | Alternative Cover Assessment Program                                |
| BC             | bound cations   |
| CEC            | cation exchange capacity  |
| CMH            | chilled mirror hygrometer   |
| CMP            | common midpoint   |
| D              | diameter  |
| DW             | deionized water   |
| ET             | evapotranspiration  |
| GCL            | geosynthetic clay liner   |
| GDL            | geosynthetic drainage layer   |
| GM             | geomembrane   |
| GPR            | ground penetrating radar  |
| H              | depth of water in outer ring of SDRI                                |
| HDPE           | high density polyethylene   |
| H <sub>b</sub> | height of water in bubbling tube in BH relative to base of borehole |
| I              | infiltration rate   |
| ICP-OES        | inductively coupled plasma – optical emissions spectrometry         |
| I <sub>s</sub> | ionic strength  |
| K              | hydraulic conductivity  |
| L <sub>f</sub> | depth of the wetting front  |
| LLDPE          | linear low density polyethylene                                     |
| MARV           | minimum average role value  |
| MDR            | charge ratio of monovalent to divalent soluble cations              |
| MFI            | melt flow index   |

|       |   |
|-------|---|
| MSW   | municipal solid waste                                 |
| OIT   | oxidation induction time                              |
| PET   | potential evapotranspiration                          |
| Q     | volumetric flow rate                                  |
| RMD   | ratio of monovalent to divalent cations in a solution |
| SC    | soluble cations                                       |
| SDRI  | sealed double-ring infiltrometer                      |
| SI    | swell index   |
| SW    | standard water (0.01 M CaCl <sub>2</sub> )            |
| SWCC  | soil water characteristic curve                       |
| TDR   | time domain reflectometry                             |
| BH    | borehole permeameter                                  |
| TCM   | total soluble cations charge per mass                 |
| USCS  | Unified Soil Classification System                    |
| USEPA | US Environmental Protection Agency                    |

### **Western Symbols**

|                   |   |
|-------------------|---|
| Ca                | calcium   |
| Cl                | chlorine  |
| K                 | potassium   |
| K <sub>F</sub>    | field-measured saturated hydraulic conductivity           |
| K <sub>s</sub>    | saturated hydraulic conductivity                          |
| K <sub>sa</sub>   | as-built saturated hydraulic conductivity                 |
| K <sub>SDRI</sub> | field-measured hydraulic conductivity with SDRI           |
| K <sub>si</sub>   | in-service saturated hydraulic conductivity               |
| K <sub>BH</sub>   | field-measured hydraulic conductivity with BH permeameter |



|          |  |
|----------|--|
| $n$      | shape parameter in van Genuchten's equation                            |
| $n_{LS}$ | shape parameter in van Genuchten's equation from large-scale tests     |
| $n_{SS}$ | shape parameter in van Genuchten's equation from small-scale tests     |
| $n_a$    | shape parameter in van Genuchten's equation from as-built test section |
| Na       | sodium   |
| Mg       | magnesium  |
| $p$      | p statistic from t-test  |
| $t$      | t statistic from t-test  |
| $X_m$    | mole fraction of monovalent cations                                    |

### **Greek Symbols**

|                 |  |
|-----------------|--|
| $\alpha$        | shape parameter in van Genuchten's equation                            |
| $\alpha_a$      | shape parameter in van Genuchten's equation from as-built test section |
| $\alpha_{LS}$   | shape parameter in van Genuchten's equation from large-scale tests     |
| $\alpha_{SS}$   | shape parameter in van Genuchten's equation from small-scale tests     |
| $\gamma_{dmax}$ | maximum dry unit weight on compaction curve                            |
| $\theta$        | volumetric water content   |
| $\theta_r$      | residual volumetric water content                                      |
| $\theta_s$      | saturated volumetric water content                                     |
| $\Theta$        | effective saturation   |
| $\sigma$        | standard deviation   |



**APPENDIX A – EXHUMATION PHOTO GALLERY**





Fig. A.1. Test field prior to decommissioning.



Fig A.2. Decommissioning weather station.

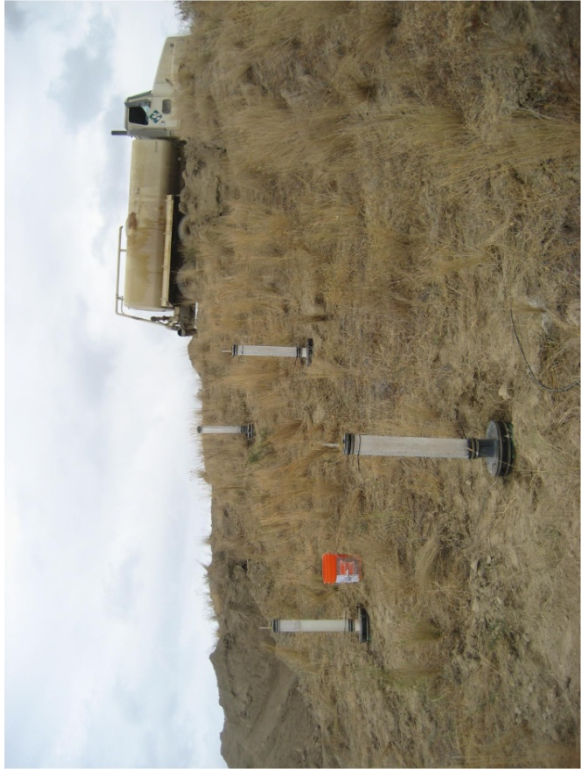


Fig A.3. Constant head TSBs in operation.



Fig A.4. Investigating soil paedogenesis.



Fig A.6. Constructed defect in GM.



Fig A.5. Sampling GDL in section with composite barrier.



Fig A.8. Delicately plating GCL to avoid disturbance.



Fig A.7. Removing GCL sample from composite barrier.



Fig A.9. Removing GCL samples from composite barrier.

**APPENDIX A.1 – EXHUMATION OF HELENA, MONTANA SITE**





Fig. A.10. Test field prior to decommissioning.



Fig. A.11. Cover soil removed prior to SDR1 installation.



Fig. A.12. Cutting trenches for SDR1 installation.



Fig. A.13. Adding granular bentonite to seal SDR1.



Fig. A.14. Filling SDRI, inner cap visible.



Fig. A.15. Constant head TSB in operation.



Fig. A.16. Excavation of block sample.



Fig. A.17. Supervision during block sample exhumation.



Fig. A.18. Removing lysimeter GDL for laboratory analysis.



Fig. A.19. Operating SDRI with constant head inner ring.

**APPENDIX A.2 – EXHUMATION OF POLSON, MONTANA SITE**



Fig. A.20. Test field (in fence) prior to decommissioning.



Fig. A.21 Digging block sample for laboratory analysis.



Fig. A.22. Macroscopic in-situ flow path.



Fig. A.23. Close-up of macroscopic in-situ flow path.



Fig. A.24 Geophysical investigation prior to excavations.



Fig. A.25. Geophysical investigation prior to excavations.



Fig. A.26. Horizontal plane of roots found during block sampling.



Fig. A.27. Close up of root plane.



Fig. A.28. Installing SDRI under GM into CCL.



Fig. A.29. Installation of SDRI seating trenches.



Fig. A.30. SDRI inner ring after assembly but prior to filling.



Fig. A.31. Digging subsurface block sample.



Fig. A.32. Vertical root planes.



Fig. A.33. Alternative (ET) cover profile, veg. barrier visible.



Fig. A.34. Sampling ET cover for water content profile.



Fig. A.35. Running SDRI in ET cover.





Fig. A.36. Failure along vertical root planes during trenching.



Fig. A.38. Location of Polson, MT ACAP test section.



Fig. A.37. Water removal from completed SDRI.

**APPENDIX A.3 – EXHUMATION OF OMAHA, NEBRASKA SITE**



Fig. A.39. ACAP signage.



Fig. A.40 Test field prior to decommissioning.



Fig. A.41. Initial geophysical investigation.



Fig. A.42. Constant head TSBs during operation.



Fig. A.43. Installing TSB, rough bottom to avoid smearing.



Fig. A.44. Grouting TSB with bentonite paste.



Fig. A.45. Installing Mariette bottle for constant head testing.



Fig. A.46. TSB data collection with narrow Mariette bottle.



Fig. A.47. Conventional cover profile (soil above GM).



Fig. A.49. In-situ water content reflectometer.



Fig. A.48. Conventional cover profile (CCL below GM).



Fig. A.50. Soil overlying GM in conventional cover (flipped).



Fig. A.51. Soil underlying GM in conventional cover.

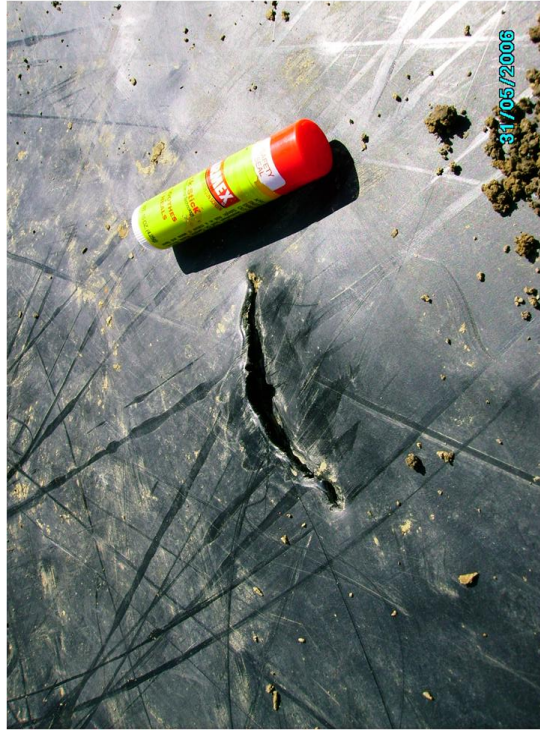


Fig. A.53 Close-up of unintentional hole from installation found via geophysical investigation.



Fig. A.52. Unintentional hole from installation found via geophysical investigation.



Fig. A.54. AO1 (Capillary barrier) cover profile.



Fig. A.55. Close up of capillary barrier in AO1.



Fig. A.57. Close-up of undisturbed roots extending across capillary barrier and into course layer in AO1.



Fig. A.56. Roots extending into course layer in AO1.



Fig. A.58. AO2 (Capillary barrier) cover profile.



Fig. A.60. Close-up of vegetation barrier in AO2.

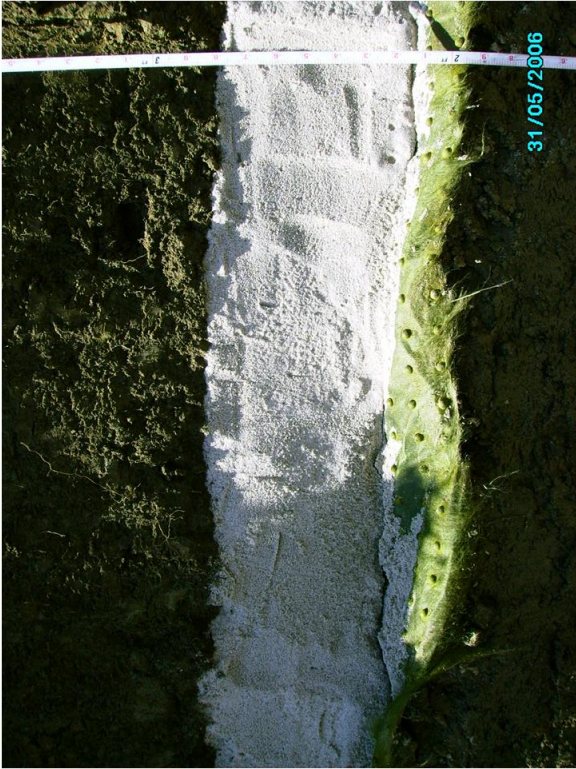


Fig. A.59. Close-up of capillary barrier in AO2.



Fig. A.61. AO2 (capillary barrier) cover profile.



**APPENDIX A.4 – EXHUMATION OF UNDERWOOD, NORTH DAKOTA SITE**



Fig. A.62. ACAP signage at Coal Creek Station.



Fig. A.63. Lysimeter and instrumentation trailer.



Fig. A.64. Interior of lysimeters and instrumentation trailer.



Fig. A.65. In situ instrumentation data logger.



Fig. A.66. Test field prior to decommissioning.



Fig. A.67. Digging block sample for laboratory analysis.



Fig. A.68. TSBs in operation, and test pits.



Fig. A.69. Mixing bentonite grout for TSB installation.



Fig. A.70. Thicker (3 ft) CCL profile (desiccated across profile).



Fig. A.71. Digging block sample in thicker CCL.



Fig. A.72. Roots visible down to veg. barrier in all profiles.



Fig. A.73. Root planes visible on ped removed from bottom of desiccated CCL.



Fig. A.74 Discussing observations with regulators.



Fig. A.75. Thicker CCL (5 ft), desiccation and roots visible throughout profile.

**APPENDIX A.5 – EXHUMATION OF MONTICELLO, UTAH SITE**



Fig. A.76. Repository marker.



Fig. A.77. Test field prior to testing.



Fig. A.78. Vegetation layer removed for SDRI installation.



Fig. A.79. Preparation of site for SDRI installation.



Fig. A.80. Measuring in-situ density prior to sampling.



Fig. A.81. Cleaning site for SDRI installation.



Fig. A.82. Sealing upper TSB section with granular bentonite.



Fig. A.83. Close-up of granular bentonite .





Fig. A.84. Constant head TSBs in operation.



Fig. A.85. Setting SDR1 in trenches.



Fig. A.86. Sealing SDR1 perimeter with granular bentonite.



Fig. A.87. Installing bentonite grout for inner TSB ring.



Fig. A.88. Installed TSB prior to operation.



Fig. A.89. Macroscopic flow path visible at bottom of TSB.



Fig. A.90. Block sample ring prior to sampling.



Fig. A.91. Removing vegetation prior to sampling.



Fig. A.92. Excavating additional soil during sampling.



Fig. A.93. Continued soil excavation for sampling.



Fig. A.94. Lower block sampling.



Fig. A.95. Trench for examination of soil structure.



Fig. A.96. Analysis of soil structure.



Fig. A.97. Re-compacting soil after sampling.



Fig. A.98. Ensuring re-compaction to initial dry density.